

Ruby pressure scale in a low-temperature diamond anvil cell

Hitoshi Yamaoka, Yumiko Zekko, Ignace Jarrige, Jung-Fu Lin, Nozomu Hiraoka et al.

Citation: *J. Appl. Phys.* **112**, 124503 (2012); doi: 10.1063/1.4769305

View online: <http://dx.doi.org/10.1063/1.4769305>

View Table of Contents: <http://jap.aip.org/resource/1/JAPIAU/v112/i12>

Published by the [American Institute of Physics](#).

Related Articles

BX90: A new diamond anvil cell design for X-ray diffraction and optical measurements
Rev. Sci. Instrum. **83**, 125102 (2012)

Oxy-acetylene driven laboratory scale shock tubes for studying blast wave effects
Rev. Sci. Instrum. **83**, 045111 (2012)

Pressure distribution in a quasi-hydrostatic pressure medium: A finite element analysis
J. Appl. Phys. **110**, 113523 (2011)

Multipurpose high-pressure high-temperature diamond-anvil cell with a novel high-precision guiding system and a dual-mode pressurization device
Rev. Sci. Instrum. **82**, 095108 (2011)

A high temperature high pressure cell for quasielastic neutron scattering
Rev. Sci. Instrum. **82**, 083903 (2011)

Additional information on *J. Appl. Phys.*

Journal Homepage: <http://jap.aip.org/>

Journal Information: http://jap.aip.org/about/about_the_journal

Top downloads: http://jap.aip.org/features/most_downloaded

Information for Authors: <http://jap.aip.org/authors>

ADVERTISEMENT



AIP Advances

Now Indexed in Thomson Reuters Databases

Explore AIP's open access journal:

- Rapid publication
- Article-level metrics
- Post-publication rating and commenting

Ruby pressure scale in a low-temperature diamond anvil cell

Hitoshi Yamaoka,¹ Yumiko Zekko,² Ignace Jarrige,³ Jung-Fu Lin,⁴ Nozomu Hiraoka,⁵ Hirofumi Ishii,⁵ Ku-Ding Tsuei,⁵ and Jun'ichiro Mizuki^{2,6}

¹Harima Institute, RIKEN (The Institute of Physical and Chemical Research), Sayo, Hyogo 679-5148, Japan

²Graduate School of Science and Technology, Kansai Gakuin University, Sanda, Hyogo 669-1337, Japan

³National Synchrotron Light Source II, Brookhaven National Laboratory, Upton, New York 11973, USA

⁴Department of Geological Sciences, The University of Texas at Austin, Austin, Texas 78712, USA

⁵National Synchrotron Radiation Research Center, Hsinchu 30076, Taiwan

⁶Japan Atomic Energy Agency, SPring-8, Sayo, Hyogo 679-5148, Japan

(Received 1 August 2012; accepted 12 November 2012; published online 17 December 2012)

Laser-excited N and R fluorescence lines of heavily doped ruby have been studied up to 26 GPa at low temperatures. While the intensity of the R lines at ambient pressure significantly decreases with decreasing temperature, the intensity of N lines originating from exchange-coupled Cr ion pairs is enhanced at low temperatures. The pressure induced wavelength shift of the N lines at 19 K is well fitted with an empirical formula similar to the equation for the R_1 line, showing that the intense N line could be used as an alternative pressure scale at low temperatures. We also observe continuous increase in non-hydrostaticity with increasing pressure at low temperatures when silicone oil and 4:1 mixture of methanol and ethanol are used as pressure media. © 2012 American Institute of Physics. [<http://dx.doi.org/10.1063/1.4769305>]

I. INTRODUCTION

Application of external hydrostatic pressure has gained increasing interest in physics over the past few decades as a clean and efficient way to change the density of materials. In semiconductor physics, many experiments under high-pressure and low-temperature conditions have been performed.^{1,2} In strongly correlated systems low temperature conditions are usually given more attention due to the occurrence of a number of highly interesting physical properties, including superconductivity and quantum critical behavior.³ Because pressure can have dramatic effects on these low-temperature properties, the combination of high-pressure and low-temperature conditions is central to condensed matter physics.

Of particular importance to a high-pressure experiment is the reliability of a pressure gauge used. Laser-induced ruby fluorescence R_1 line has most commonly been used as a pressure gauge for pressure determinations up to Mbar range.^{4–11} The R_1 and R_2 fluorescence lines (694.2 and 692.81 nm, respectively) are separated by a crystal field splitting of the 2E_g level of the Cr^{3+} ions in a corundum (Al_2O_3) lattice. Utilization of linear red shift of the ruby fluorescence R_1 line (${}^2E_g \rightarrow {}^4A_{2g}$ emission following ${}^4A_{2g} \rightarrow {}^4T_{2g}$ or ${}^4T_{1g}$ excitation) as a function of pressure to 2.3 GPa was first showed by Forman *et al.*⁴ Mao *et al.* introduced a nonlinear calibration at higher pressures.^{8,9} Temperature-dependent fluorescence shift had been measured for the R lines.^{11–21} These studies reported the shift, splitting, and width of the R_1 and R_2 lines as a function of temperature. Only small changes in both the shift and the line width were reported at $T < 100$ K.^{12,14,17,21} In contrast, the intensity ratio of the two R lines has been suggested as a potential thermometer over the range 10–100 K.¹⁵ However, very few studies have been

carried out to examine the pressure-induced shift of the R lines at low temperatures above 10 GPa.^{20,22} The shift of the R_1 lines has been calibrated using NaCl pressure scale up to 22 GPa and temperatures at 10 and 77 K.²² Slight deviations of the R_1 shift from the calibrated function at room temperature (RT)^{8,11} were also reported at 4.5 K.²⁰

It has been shown that increasing Cr-doping level in the ruby enhances not only the intensity of the R lines but also that of the two N lines,^{23–26} which are attributed to the second (N_1 , 4A_1) and fourth (N_2 , 3A_2) nearest neighbor pairs of the Cr^{3+} ions.²⁶ These N lines originate from the exchange coupled pairs of the Cr^{3+} ions. The colors of the ruby are, respectively, colorless, pink-like, red-like, and grey in visible light for the Cr-concentration of much less than 0.1%, about 0.1%, about 1%, and more than 5%. The temperature-dependent N -line spectra were also investigated, showing a similar trend for the R lines except for the intensity.^{26–29} While the intensity of the R lines was significantly reduced by a few orders of magnitudes,^{29,30} the N lines were found to gain intensity at low temperatures.^{26,27} With the Cr^{3+} concentration below 0.1% only two R lines from isolated Cr^{3+} ions were observed. The N -line intensity increases with the Cr-doping concentration, although not linearly, reflecting both the increase of the formation probability of paired ions and the energy transfer from single ions to paired ions. Increasing the Cr-concentration above 1% causes a broad-band emission as a result of the formation of the Cr^{3+} ion clusters.

To date, the pressure dependence of the N lines at low temperatures has not been reported. Furthermore, only a few quantitative studies have been reported on the hydrostaticity of the pressure mediums at low temperatures.^{31,32} In this paper, we study the temperature and pressure dependences of the N spectrum of heavily doped ruby, along with the R lines for comparison, at 19 and 65 K and pressures up to 26 GPa.

Our results show that the intensity of the N lines is much higher than that of the R_1 line and shifts with pressure in a similar fashion to R_1 at low temperatures. This indicates that the N line could be used as a reliable alternative secondary pressure scale in the low-temperature high-pressure range where the R_1 line is too weak to be properly detected. At low temperatures, we observed non-hydrostatic effects even at ambient pressure for both silicone oil and the 4:1 methanol-ethanol mixture, while at room temperature, these media retain hydrostaticity up to about 10 GPa.^{32,33}

II. EXPERIMENTS

A closed-circuit He cryostat at the beamline BL12XU of the SPring-8 is used for the low-temperature measurements from 300 K to 16 K.³⁴ High-pressure conditions are achieved using a gas-membrane controlled diamond anvil cell (DAC) equipped with 0.4-mm culet diamonds. We use a stainless-steel gasket with silicone oil as pressure-transmitting medium and a Be gasket with a 4:1 mixture by volume of methanol and ethanol in two separate experiments, respectively. The diameter of the sample chamber in the gasket is about 180 μm . Be gaskets are often used in the in-plane geometry where both incoming and outgoing x-ray beams pass through the gasket because of the higher x-ray transmissivity compared to higher- Z materials. We note that Be gaskets become increasingly brittle at lower temperatures, which limits the achievable pressures at low temperatures. Pressure is measured using the ruby R_1 lines at low temperatures. As shown below, the intensity ratio of R_1 to N_1 is about 0.5 at 77 K, indicating that the weight percentage of the doped- Cr_2O_3 is estimated to be on the order of 1%, corresponding to a heavily doped case.²⁶ A green diode laser (Laser Quantum DL532-10) with a wavelength of 532 nm is used to excite the fluorescence lines. Ruby fluorescence spectra are measured with a spectrometer (STR500-3 Raman Imaging Spectrometer) having a grating of 600 lines/mm; the system is calibrated using the emission lines of a Ne lamp. The DAC system is set in the hutch of the beamline. The fluorescence measurement are performed outside the hutch using optical fibers connected to the DAC system. For the pressure-dependent measurements, we first adjust the temperature at ambient pressure and then apply the pressure while keeping the temperature constant.

III. CALIBRATION CURVES FOR RUBY R LINE SHIFT

A number of empirical calibration curves of the R_1 fluorescence shift at high-pressures and temperatures have been proposed for the ruby pressure scale:

$$P(\text{GPa}) = \frac{A}{B} \left[\left(\frac{\lambda}{\lambda_0} \right)^B - 1 \right] \quad \text{at RT}, \quad (1)$$

$$P(\text{GPa}) = 2.76\Delta\lambda(\text{nm}) \quad \text{at 77 K}, \quad (2)$$

$$P(\text{GPa}) = 2.74\Delta\lambda(\text{nm}) \quad \text{at 10 K}, \quad (3)$$

$$P(\text{GPa}) = A_0(\text{GPa}) \ln \left(\frac{\lambda}{\lambda_0} \right) \quad \text{at 4.5K}, \quad (4)$$

where λ and λ_0 are wavelengths of the R_1 line at $P > 0$ GPa and $P = 0$ GPa, respectively, $\Delta\lambda (= \lambda - \lambda_0)$ is the wavelength shift, and A and B are constants. At RT, many calibration curves have been proposed.¹¹ Here we representatively use Eq. (1) with $A = 1904$ and $B = 7.715$.⁹ Equations (2) and (3) were derived from ruby R_1 shift using NaCl up to 22 GPa with a nitrogen pressure medium.²² The bulk modulus of NaCl was assumed independent of temperature in the equation of state used. Equation (4) was derived from the lattice parameters of silver at 4.5 K in a helium pressure medium.²⁰ A_0 was estimated to be 1762 ± 13 GPa. Calibrated pressure as a function of the ruby R_1 fluorescence shift from equations are plotted in Fig. 1.

Based on these calibrations, pressures at low temperatures are systematically lower than the pressures provided by using the formula for room temperature. For example, when $A_0 = 1762$ GPa for Eq. (4), the difference in the calculated pressures using Eqs. (1) and (4) is estimated to be about 4 GPa for a given wavelength shift of 11.6 nm (corresponding to the pressure about 30 GPa). The difference in the estimated pressures between room and low temperatures can be very significant at high pressures. We note that the difference between estimated pressures using Eqs. (2) and (3) is small, and is also reasonably small between Eqs. (2) and (4); less than 1 GPa for a given wavelength shift of 11 nm. This reflects the smaller R shift in wavelength below 100 K. In this study we calibrate the pressure at 16, 19 and 65 K from the shift of the R_1 line using Eq. (4) at 4.5 K and assuming $A_0 = 1762$.²⁰ But A_0 may have a weak temperature dependence even at these low temperatures, although the deviation from the actual values may be much less than 1 GPa as discussed above. Thus, the pressure coefficients for the N lines may have a related additional uncertainty. In the future, this parameter should be calibrated at low temperatures by x-ray diffraction measurements of lattice constants, for the NaCl calibrant as a function of pressure.

IV. RESULTS AND DISCUSSION

Figure 2 shows an example of the temperature dependence of the ruby fluorescence spectra. A stainless-steel

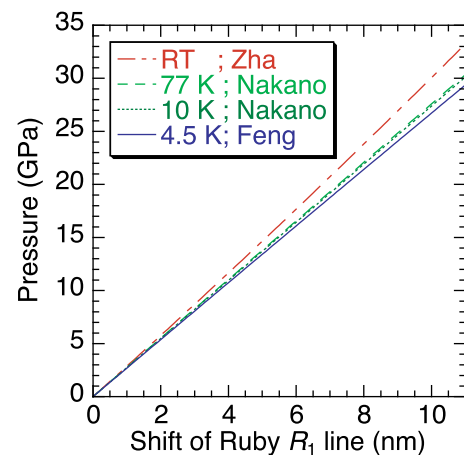


FIG. 1. Ruby R_1 fluorescence shift as a function of pressure. These lines are plotted from four different empirical formula.^{9,20,22} $A = 1868$ GPa and $B = 7.715$ in Eq. (1) and $A_0 = 1762$ in Eq. (4) are used.^{9,20}

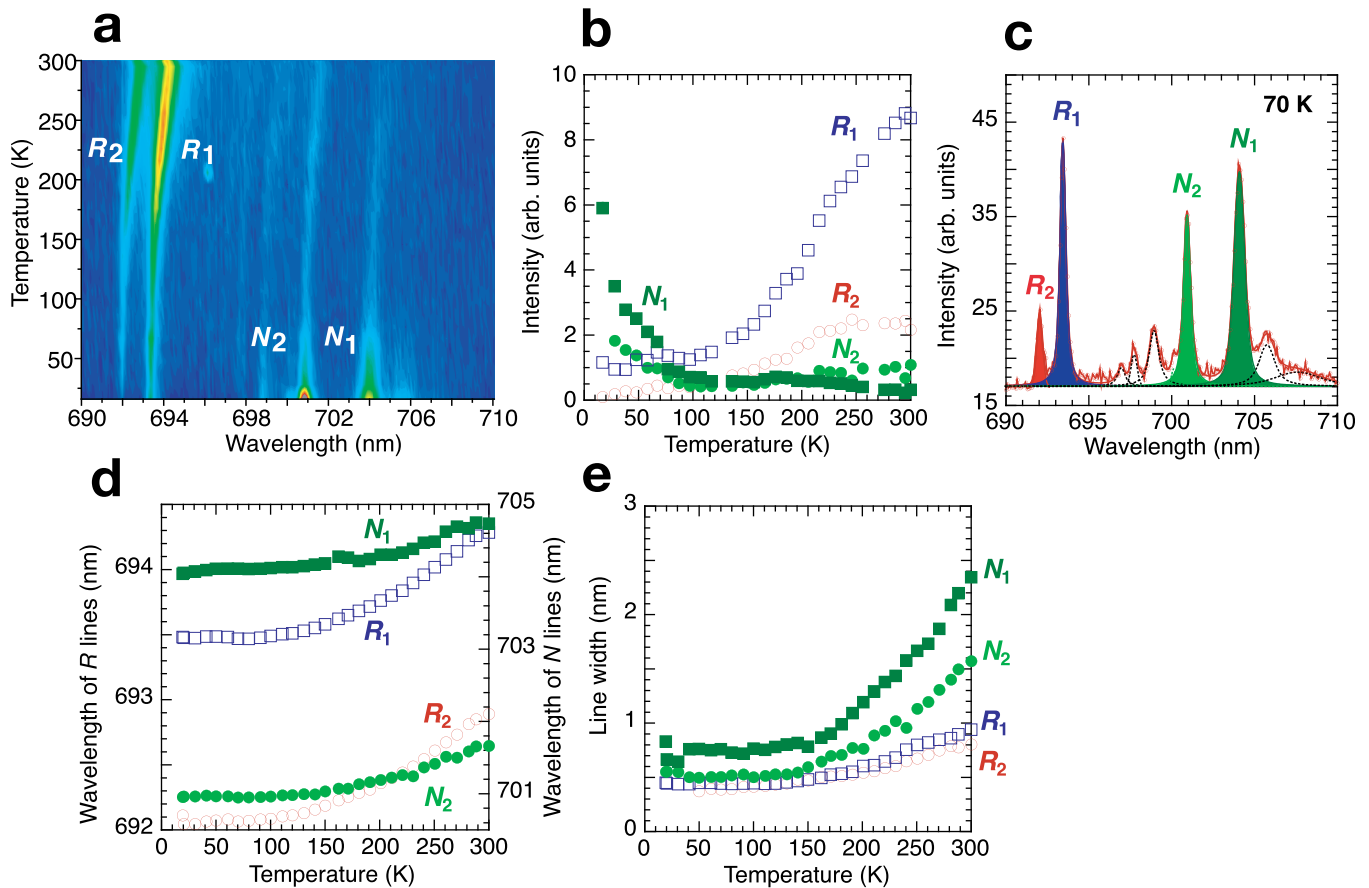


FIG. 2. Temperature dependence of ruby spectra at ambient pressure with silicone oil as pressure medium. (a) Contour map of the intensity, (b) each line intensity as a function of temperature, (c) a representative spectrum with fits at 70 K, (d) wavelengths of R and N lines, and (e) widths (FWHM) of R and N lines.

gasket is used with silicone oil as pressure-transmitting medium. For the pressure-medium consisting of a 4:1 methanol-ethanol mixture, the same temperature-induced changes in the ruby fluorescence are observed. The intensity of the R lines rapidly decreases with decreasing temperature, while that of the N lines are enhanced at low temperatures as shown in Figs. 2(a) and 2(b). The intensity of the R_2 line is significantly weaker at low temperatures as compared to that of the R_1 line as shown in Figs. 2(a) and 2(b). Since the intensity ratio of R_1 to N_1 increases with Cr-concentration, the origin of the N lines is attributed to the presence of coupled pairs of the Cr^{3+} ions.^{23,24} Figure 2(c) shows an example of the fit using Voigt functions. The temperature-induced change in the intensity ratios of the R (R_1 , R_2) to N (N_1 , N_2) lines has already been discussed.^{28,29} These intensity ratios were well fitted with an exponential curve at temperatures above 50–100 K, however, a large deviation from the curve occurred at low temperatures. This indicates thermal equilibrium of the population of the excited states at high temperatures. The temperature-induced change in the intensity of the N_1 and N_2 lines was observed to reach a maximum intensity at 55 and 25 K, respectively, with further decreasing temperature.²⁶ It is conceivable that these maxima are shifted to lower temperatures in our measurements, which could be due to a slight difference in the Cr-concentration of the ruby spheres used. In Fig. 2(e), the full width at half-maximum

(FWHM) of the R and N lines is shown. Our results are consistent with previous studies^{28,29} overall.

The intensity of both N lines increases at low temperatures in contrast to the R -line. This temperature-induced behavior of the N lines can be explained by the population derived from the ground state exchange splitting.¹³ A simple model, taking into account the energy transfer from the Cr^{3+} single ions to the exchanged coupled-pairs, described this temperature-dependent phenomenon well.³⁰ Because the intensity of the R lines is fairly weak at low temperatures, we propose that the ruby N line with enhanced intensity at low temperatures can be used as an alternative pressure gauge.

In Fig. 3, we summarize three series of measurements at low temperatures for the N and R lines. Spectra in (a-d) and (e-h) are, respectively, measured at 65 K and 19 K using the stainless-steel gasket and the silicone oil as pressure-medium. Spectra in (i-l) are obtained at 16 K with the Be gasket and the 4:1 methanol-ethanol mixture as the pressure-medium. Contour intensity maps in Figs. 3(a), 3(e) and 3(i) show the intensity rapidly decreases at high pressures. Each line intensity in Figs. 3(b), 3(f) and 3(j) shows a complex behavior as a function of pressure while overall decreasing, and we do not understand the origin of this behavior at present. Pressure is estimated from the R_1 line shift using Eq. (4) with $A_0 = 1762$. Then the shift of the N_1 and N_2 lines are plotted for these pressures, as shown in Figs. 3(c), 3(g) and

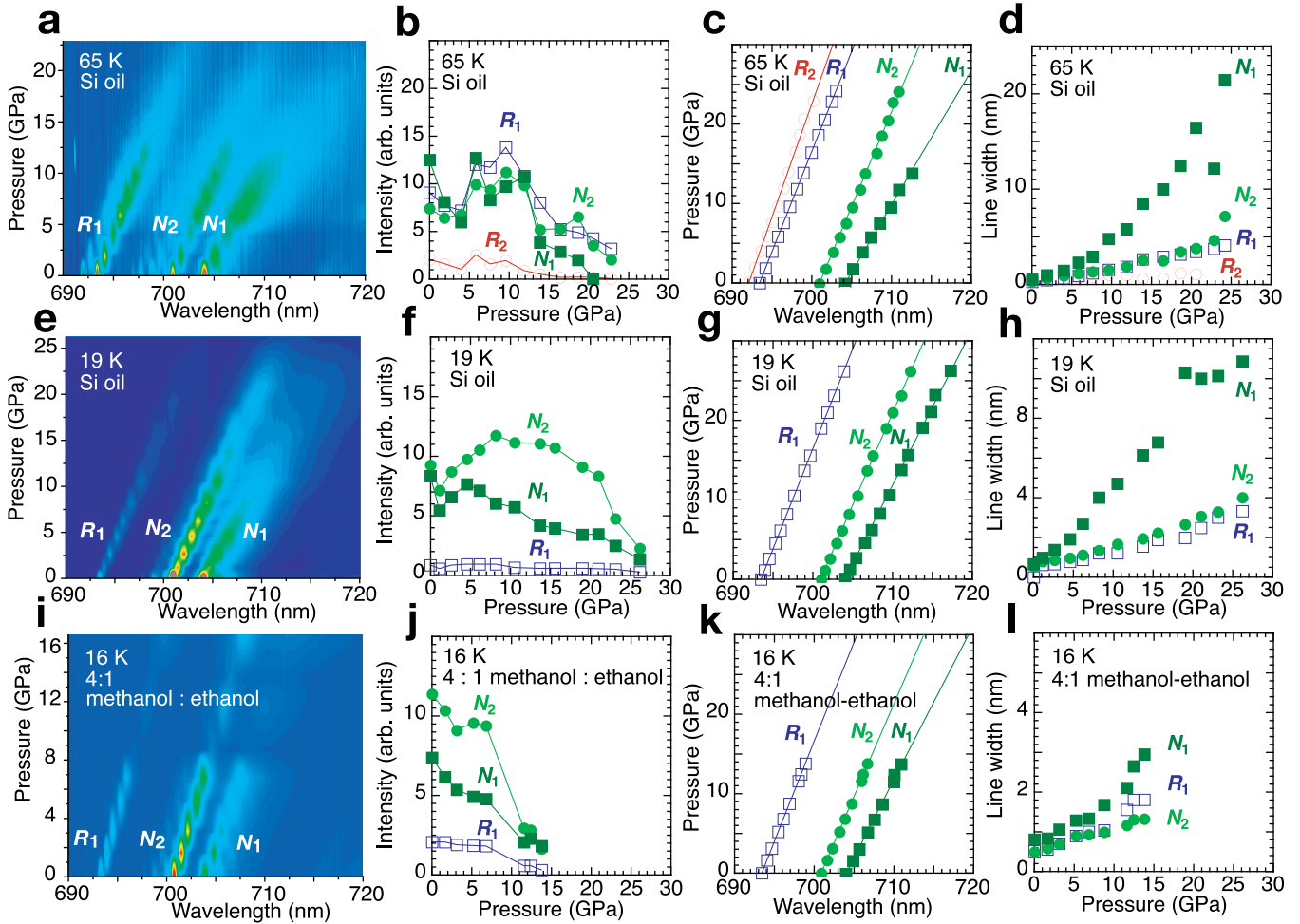


FIG. 3. Pressure-dependent ruby spectra (a)–(d) 65 K, (e)–(h) 19 K, and (i)–(l) 16 K. Silicone oil and 4:1 mixture of methanol-ethanol are used as the pressure-transmitting media in (a)–(h) and (i)–(l), respectively. (a), (e), and (i) are 2-D contour intensity maps of the ruby spectra as a function of pressure. Spotty structures such as the ones in red dots are an artifact due to the lack of the data between the measured points. (b), (f), and (j) show each line intensity as a function of pressure. (c), (g), and (k) show the relation between the peak wavelength of the R and N lines and pressure. Solid lines are fits using Eq. (4). (d), (h), and (l) shows the width (FWHM) of R and N lines as a function of pressure.

3(k) at 65, 19, and 16 K, respectively. These line shifts are well fitted with Eq. (4) up to about 26 GPa. We note that the coefficient A_0 for the N lines summarized in Table I shows a temperature dependence; it becomes smaller at low temperature. The slopes of the R and N_2 lines are nearly the same as shown in Figs. 3(c), 3(g) and 3(k), while that of N_1 is more slanted. At room temperature, a linear pressure dependence in the separation of N lines from R_1 line was also reported up to 11 GPa.³⁵ We observe that this relation holds between the R_1 and N_2 lines at low temperatures. No difference between the two pressure-transmitting media is observed within the accuracy of our measurements.

At high-pressures for the N_2 line, the FWHM is narrower and the peak intensity smaller compared with the N_1 line. In our measurements, the broadening of the ruby fluorescence reflects both inhomogeneous pressure distribution and uniaxial stress pressure. What we measure is a spatial average of these effects. Jamison and Imbusch proposed a simple model for temperature dependence of the fluorescence from heavily doped ruby taking into account excitation transfer between the clusters of chromium ions and the single chromium ions.³⁰ Based on this model, our results may indicate the

decrease of radiative and excitation transfer rates between the single and pair Cr^{3+} ions at high pressures due to the increase of the level-splitting with pressure. Figures 3(d), 3(h) and 3(l) show rapid increase of the FWHM of the N_1 line with pressure, but the increase of the width in the N_2 and R_1 lines is relatively low. At present, the origin of this difference

TABLE I. Coefficient A_0 in Eq. (4) for the ruby fluorescence R and N lines. Error for A_0 is about ± 20 GPa.

T (K)	Pressure medium	Gasket	Line	A_0 (GPa)
65	Silicone	Stainless	R_1	1762
			R_2	1985
			N_1	1685
			N_2	1203
19	Silicone	Stainless	R_1	1762
			N_1	1635
			N_2	1399
16	4:1 Methanol-ethanol	Be	R_1	1762
			N_1	1625
			N_2	1373

remains unclear and merits further study. The excitation of the R lines with a green laser is inefficient at high pressures due to the blue shift of the U (4T_1) and Y (4T_2) absorption bands to high energy.^{36,37} Alternatively, the R line excitation using a red laser excitation via the 2T_1 levels instead of the 4T_1 or 4T_2 level is preferred to enhance the intensity of R and N lines.^{11,37} When a green laser is used for the excitation of the ruby fluorescence lines and the R_1 line has vanished at high pressures, the stronger N_2 line can then be conveniently used as a substitute pressure gauge for higher pressures until it vanishes. The FWHMs of all lines increase constantly with pressure.

The hydrostaticity of the pressure-transmitting medium has been previously discussed based on the broadening of the emission lines.³⁸ We note that the hydrostatic limit is around 10 GPa for the 4:1 mixture of methanol-ethanol at room temperature.³³ Our results indicate that at low temperatures the non-hydrostatic effect develops continuously starting at ambient pressure. Viscosity and elastic behavior of silicone oil are similar to the 4:1 methanol-ethanol mixture.³⁹ It is known that the silicone oil does not depart from hydrostaticity up to 10 GPa, and its hydrostaticity remains overall higher than that of the alcohol mixture at room temperature.⁴⁰ On the other hand, at 77 K, the 4:1 methanol-ethanol mixture showed less non-hydrostatic effects compared with other media such as silicone oil.³⁸ Our results at 16–19 K show that the difference of non-hydrostaticity between the 4:1 methanol-ethanol mixture and silicone oil is small at low temperatures.

V. SUMMARY

We measure the temperature and pressure dependences of the laser-induced ruby fluorescence N with the R lines for the heavily doped ruby in DAC. The intensity of the R lines from heavily doped ruby becomes weaker with decreasing temperature, while the N lines does stronger at $T < 50$ K. The stronger N lines at low temperatures below a few tens K may be used to replace the much weaker R lines for pressure scaling. We confirm the empirical formula at low temperatures for the relation between the ruby shift of the N lines at pressures up to 14 GPa for the 4:1 methanol-ethanol mixture and up to 26 GPa for the silicone oil, respectively. At low temperatures, non-hydrostaticity develops at a constant rate at ambient pressure. The difference of the non-hydrostatic effect between the 4:1 methanol-ethanol mixture and silicone oil is small at low temperatures.

ACKNOWLEDGMENTS

The experiments were performed at Taiwan beamline BL12XU, SPring-8, partly under an approval of JASRI (Proposals Nos. 2011B4259 and 2011B4265) and NSRRC, Taiwan (2010-3-011, 2012-1-013). This work is partly supported by a Grant in Aid for Scientific research (Kiban C No. 22540343 and Kiban A No. 22244038) from the Japan Society for the Promotion of Science. J.F.L. acknowledges support from the Energy Frontier Research under Extreme Environments (EFree), the US National Science Foundation

(EAR-0838221) and the Carnegie/DOE Alliance Center (CDAC). We also appreciate Nikki Seymour for the manuscript.

- ¹A. R. Goñi, A. Cantarero, K. Syassen, and M. Cardona, *Phys. Rev. B* **41**, 10111 (1990).
- ²A. Mang, K. Reimann, and St. Rübenacke, *Solid State Commun.* **94**, 251 (1995).
- ³H. Yamaoka, I. Jarrige, N. Tsujii, J.-F. Lin, T. Ikeno, Y. Isikawa, K. Nishimura, R. Higashinaka, H. Sato, N. Hiraoka, H. Ishii, and K.-D. Tsuei, *Phys. Rev. Lett.* **107**, 177203 (2011).
- ⁴R. Forman, G. J. Piermarini, J. D. Barnett, and S. Block, *Science* **176**, 284 (1972).
- ⁵J. D. Barnett, S. Block, and G. J. Piermarini, *Rev. Sci. Instrum.* **44**, 1 (1973).
- ⁶H. K. Mao and P. M. Bell, *Science* **191**, 851 (1976).
- ⁷H. K. Mao, P. M. Bell, J. W. Shaner, and D. J. Steinberg, *J. Appl. Phys.* **49**, 3276 (1978).
- ⁸H. K. Mao, J. Xu, and P. M. Bell, *J. Geophys. Res.* **91**, 4673, doi:10.1029/JB091iB05p04673 (1986).
- ⁹C.-S. Zha, H.-K. Mao, and R. J. Hemley, *Proc. Nat. Acad. Sci. U.S.A.* **97**, 13494 (2000).
- ¹⁰I. F. Silvera, A. D. Chijioko, W. J. Nellis, A. Soldatov, and J. Tempere, *Phys. Status Solidi. B* **244**, 460 (2007).
- ¹¹K. Syassen, *High Press. Res.* **28**, 75 (2008).
- ¹²D. E. McCumber and M. D. Sturge, *J. Appl. Phys.* **34**, 1682 (1963).
- ¹³J. P. van der Ziel, *Phys. Rev. B* **9**, 2846 (1974).
- ¹⁴I. F. Silvera and R. J. Wijngaarden, *Rev. Sci. Instrum.* **56**, 121 (1985).
- ¹⁵B. A. Weinstein, *Rev. Sci. Instrum.* **57**, 910 (1986).
- ¹⁶W. L. Vos and J. A. Schouten, *J. Appl. Phys.* **69**, 6744 (1991).
- ¹⁷D. D. Ragan, R. Gustavsen, and D. Schiferl, *J. Appl. Phys.* **72**, 5539 (1992).
- ¹⁸A. H. Jahren, M. B. Kruger, and R. Jeanloz, *J. Appl. Phys.* **71**, 1579 (1992).
- ¹⁹X. Li-Wen, C. Rong-Zheng, and J. Chang-Qing, *Chin. Phys. Lett.* **17**, 555 (2000).
- ²⁰Y. Feng, R. Jaramillo, J. Wang, Y. Ren, and T. F. Rosenbaum, *Rev. Sci. Instrum.* **81**, 041301 (2010).
- ²¹D. M. Adams, R. Appleby, and S. K. Sharma, *J. Phys. E: Sci. Instrum.* **9**, 1140 (1976).
- ²²K. Nakano, Y. Akahama, Y. Ohishi, and H. Kawamura, *Jpn. J. Appl. Phys., Part 1* **39**, 1249 (2000).
- ²³J. C. Chervin, B. Canny, and M. Mancinelli, *High Press. Res.* **21**, 305 (2001).
- ²⁴A. L. Schawlow, D. L. Wood, and A. M. Clogston, *Phys. Rev. Lett.* **3**, 271 (1959).
- ²⁵A. L. Schawlow, *J. Appl. Phys. Suppl.* **33**, 395 (1962).
- ²⁶G. F. Imbusch, *Phys. Rev.* **153**, 326 (1967).
- ²⁷R. C. Powell, B. DiBartolo, B. Birang, and C. S. Naiman, *J. Appl. Phys.* **37**, 4973 (1966).
- ²⁸R. C. Powell, B. DiBartolo, B. Birang, and C. S. Naiman, *Phys. Rev.* **155**, 296 (1967).
- ²⁹R. C. Powell and B. DiBartolo, *Phys. Status Solidi A* **10**, 315 (1972).
- ³⁰S. P. Jamison and G. F. Imbusch, *J. Lumin.* **75**, 143 (1997).
- ³¹H. Fukazawa, K. Hirayama, T. Yamazaki, Y. Kohori, and T. Matsumoto, *J. Phys. Soc. Jpn.* **76**, 125001 (2007).
- ³²N. Tateiwa and Y. Haga, *Rev. Sci. Instrum.* **80**, 123901 (2009).
- ³³S. Klotz, J.-C. Shervin, P. Munsch, and G. Le Marchand, *J. Phys. D: Appl. Phys.* **42**, 075413 (2009).
- ³⁴H. Yamaoka, I. Jarrige, N. Tsujii, J.-F. Lin, N. Hiraoka, H. Ishii, and K.-D. Tsuei, *Phys. Rev. B* **82**, 035111 (2010).
- ³⁵Q. Williams and R. Jeanloz, *Phys. Rev. B* **31**, 7449 (1985).
- ³⁶S. J. Duclos, Y. K. Vohra, and A. L. Ruoff, *Phys. Rev. B* **41**, 5372 (1990).
- ³⁷N. H. Chen and I. F. Silvera, *Rev. Sci. Instrum.* **67**, 4275 (1996).
- ³⁸N. Tateiwa and Y. Haga, *J. Phys.: Conf. Ser.* **215**, 012178 (2010).
- ³⁹D. D. Ragan, D. R. Clarke, and D. Schiferl, *Rev. Sci. Instrum.* **67**, 494 (1996).
- ⁴⁰Y. Shen, R. S. Kumar, M. Pravica, and M. F. Nicol, *Rev. Sci. Instrum.* **75**, 4450 (2004).